WILEY | Hindawi

Research Article

Fluidity Influencing Factors Analysis and Ratio Optimization of New Sealing Materials Based on Response Surface Method

Xin Guo [iD],[1] Sheng Xue [iD],[1] Yaobin Li [iD],[1] Chunshan Zheng [iD],[1] and Gege Yang[2]

[1]*School of Safety Science and Engineering, Anhui University of Science & Technology, Huainan 232001, China*
[2]*School of Management Studies, Shanghai University of Engineering Science, Shanghai 201620, China*

Correspondence should be addressed to Xin Guo; guoxin190510@163.com

The borehole sealing material is one of the key factors affecting the gas drainage effect of a borehole. This paper takes the compressive strength, fluidity, expansion rate, and setting time of the sealing material as the main research indicators and explores the influence of each key influencing factor on the performance of the high-fluid sealing material through the single factor experiment method. Using the Design-Expert 8.0.5 Trial software designed orthogonal experiments and establishing a quadratic model between liquidity and each test factor, which showed the impact of each key factor on the fluidity. Finally, by adjusting the amount of admixtures, the optimal ratio of high-fluidity borehole sealing materials was obtained. The results showed that the key factors had the following order of significance: water – cement reducing agent > water – cement ratio > retarder > expansion agent. With the water-cement ratio and the amount of water reducing agent increase, the fluidity of the material will increase; and with the increase of the retarder and expansion agent, the fluidity will decrease. In actual use, the fluidity is the main factor, but the expansion rate, compressive strength, and setting time are also considered. The optimal percentages were found for the high-fluidity borehole sealing material: a water-cement ratio of 1, along with 0.03% retarder, 0.5% water reducer, and 8% expansion agent. These research results could provide a reference for improving the performance of gas drainage borehole sealing materials and enhancing the effect of gas drainage.

1. Introduction

China has a high frequency of gas disaster accidents. With the increasing mining depth of coal resources, China is faced with increasingly serious gas problems, which pose a serious threat to the safety and efficiency of coal mining [1–3]. In order to prevent gas accidents during coal mining, gas predrainage technology is usually used to extract the gas from coal seams. However, the effect of gas drainage in China is generally poor. In addition to the low air permeability of the coal seam, the performance of the borehole sealing material also affects the drilling and sealing effect to a large extent. The borehole sealing materials commonly used in China's coal mines include cement mortar and polyurethane materials. However, these materials have poor penetration in microfissures smaller than 0.1 mm, and the cracks are closed under high stress [4], resulting in poor sealing effects. This requires a borehole sealing material with good fluidity to

allow it to be effectively injected into the fine cracks in the coal and rock mass [5, 6]. Ultrafine cement prepared by refining ordinary cement particles can meet the injection requirements for fine cracks. Compared with traditional borehole sealing materials, ultrafine cement materials have higher strength, better durability, and nontoxicity [7–9]. However, to ensure that the borehole sealing material can be efficiently injected into the fine cracks of the coal and rock mass, in addition to having high fluidity, it should also have relatively high stability, a certain degree of microswelling, and a suitable setting time [10].

Scholars in China and abroad have conducted numerous studies on ultrafine cement. Li et al. [11] developed an improved construction solid waste cement grouting material. The results show that when the mixing amount of modified construction solid waste cement grouting material waste red brick powder is 40-60%, the fluidity performance of grouting sealing material is the best. Zheng et al. [12] studied

TABLE 1: Chemical composition of raw materials/%.

Chemical composition	w (SiO$_2$)	w (Al$_2$O$_3$)	w (Fe$_2$O$_3$)	w (CaO)	w (MgO)	w (SO$_3$)	Loss	Total
HCSA expanding agent	4.96	8.52	0.99	64.18	2.67	16.97	1.19	99.48
Superfine Portland cement	20.57	9.89	3.08	57.65	2	2.7	2.6	98.49

TABLE 2: Single-factor experimental design scheme.

Test group	Water–cement ratio			Retarder			Water–reducing agent			Expanding agent		
Level/%	0.8	1.0	1.2	0.05	0.5	1.5	0.2	0.5	0.8	5	10	15

TABLE 3: Value range of each factor in orthogonal experiment.

| Test group | Value range of each factor/% | | | |
	Water–cement ratio	Retarder	Water–reducing agent	Expanding agent
ZJ1-29	0.8–1.0	0.03–0.05	0.3–0.5	8–10

FIGURE 1: Borehole sealing material after mixing.

FIGURE 2: Preparation of sample.

the effect of fly ash on the rheological properties of cement slurry. When the content of fly ash was 50%, the viscosity of cement slurry decreased by 54%, and the fluidity was improved. When the fly ash content reaches 70%, the cement slurry shows the characteristics of the Bingham fluid model. Liu et al. [13] studied the effect of nanoscale viscosity regulator on the rheological properties of cement slurry. With the incorporation of nanoscale viscosity regulator, the fluidity of cement slurry decreased significantly. Chen et al. [14] studied the fluidity of ordinary cement materials with differ-ent amounts of ultrafine cement. Wongkornchaowalit and Lertchirakarn [15] studied the influence of polycarboxylic acid superplasticizer content on the fluidity of Portland cement. The results show that when the dosage of polycar-boxylate superplasticizer is 1.8%–2.4%, the fluidity of exper-imental cement increases greatly. Kazuki et al. [16] studied the effect of the molecular structure of superplasticizer on the fluidity of cement slurry sealing material. The results show that the smaller molecular structure is helpful to the dispersion of cement particles and improves the fluidity of slurry sealing material. Güllü et al. [17] studied the influence of geopolymer grouting material on the rheological proper-ties of cement slurry. The rheological property of cement slurry decreases with the increase of the water/binder ratio. When the ratio of fly ash and geopolymer aggregate is 30%–40%, the rheological property of cement slurry is close to that of natural cement.

At present, the research on the modification of sealing materials is based on ordinary cement materials, which can-not be effectively filled into the fine cracks. The research on ultrafine cement materials is relatively concentrated in the repair of water conservancy, dams, foundations, and concrete engineering. Few studies have been conducted on the injected body with the characteristics of soft and broken rock, high ground pressure, and difficulty in injecting grout. Moreover, the research did not conduct comprehensive research on the composition, structure, and performance of the material, did not find a modification method that takes into account both high fluidity and super early strength, and did not develop a series of high fluidity and super early strength performance of grouting material. This research uses ultrafine silicate ultramud as the basic material and adds calcium oxide-calcium sulfate composite material as an expansion agent, and polycarboxylic acid as a water reducer and retarder, thereby developing a new type of drilling sealing material, considering the compressive strength, fluidity, and swelling rate of the material (the swelling rate of the test block after 60 days of curing). As a basis for judgment, the single factor test method and orthogonal test method are used to deter-mine the best admixture and water quality ratio.

2. Materials and Methods

2.1. Experimental Materials. The new type of borehole sealing material was based on ultrafine Portland cement. The ultra-fine cement used in the experiment was produced by Shan-dong Kangjing New Material Technology. The appearance

Figure 3: Cement fluidity test.

Figure 4: Determination of setting time.

Figure 5: Compressive strength test.

was a gray powder. The measured D90 value was 12.6 μm, and the measured D50 value was 5 μm. In addition, all the technical parameters and indicators met the requirements of "Superfine Portland Cement" (GB/T35161-2017). Its chemical composition is provided in Table 1. The expansion agent used in this experiment was a calcium oxide-calcium sulfate composite expansion agent (HCSA) produced by Shijiazhuang City Functional Building Materials Co., Ltd., and it had the appearance of an off-white powder. Its components are listed in Table 1. The polycarboxylic acid water-reducing agent (PCE) used in the experiment was produced by Fuyang Chengnan Building Materials Co., Ltd. It was a white powder that was easily soluble in water, and the water reduction rate was 20-35%. The retarder used in this experiment was seaweed powder produced by Jiangsu Changzhou Angu Waterproof Material Co., Ltd. The seaweed powder

had the appearance of a white powder and was easily soluble in water. The solution was a colorless and transparent viscous liquid. Water was used to formulate a solution with a mass ratio of 1 : 130.

2.2. Experimental Method. Researchers have found that the addition of a retarder [18] and HCSA [19–21] will help cement hydration products to form a good spatial structure and improve the strength of cement, while the addition of PCE has a dispersing effect on cement particles and can improve the workability of cement and reduce unit water consumption [22, 23]. In a case where the interaction of various additives to the ultrafine cement and their influences on its strength and expansibility are unknown, the single factor experiment method can be used in preliminary experiments to determine the optimal dosage ranges. Then, based on an analysis of the results, the Design-Expert 8.0.5 Trial software can be used to design an orthogonal experiment in order to accurately understand the influence of each factor on the performance of a composite expansion borehole sealing material [24–26]. In this study, after the completion of the orthogonal experiment, the Design-Expert 8.0.5 Trial software was used to calculate the variance and range of the experimental data, and the influence of the compound incorporation of various additives on the performance of the borehole sealing material was studied. Finally, a response surface regression analysis was performed on the results of the orthogonal experiment, and a quantitative regression model reflecting the relationship between the compound dosing amount of the admixture and each filling performance index was obtained, which provided a basis for the optimization of the borehole sealing material formulation.

In the experiment, the standard triple test mold (70.7 mm × 70.7 mm × 70.7 mm) was first prepared. Then, the dry material and water quantities required for the production of the test piece were calculated according to the proportions in Tables 2 and 3. After mixing with water, the weighed ultrafine cement, expansion agent, and water-reducing agent were added together and mixed thoroughly (Figure 1). Finally, water was added for thorough mixing and pouring into the mold (Figure 2), which was placed in the curing box for curing (temperature 20 ± 2°C, humidity above 95%).

The fluidity test of the borehole sealing material was conducted using the specified determination method for cement mortar fluidity (GB/T2419-2005), which was expressed by the diffusion diameter (mm) of the slurry on a horizontal glass plate. The truncated cone mold had an upper mouth diameter of 36 mm, a lower mouth diameter of 60 mm, and a height of 60 mm. The evenly stirred cement slurry was placed in a round mold, the surface was flattened, and the round mold was quickly lifted off. After the cement slurry flowed, the average of the two perpendicular diameters was measured as the maximum fluidity (Figure 3).

The standard cement consistency water consumption, setting time, and stability test method (GB/T1346—2011) was used to measure the setting time. Use cement slurry standard consistency setting time tester (Vicat meter) to measure setting time. First, zero the Vicat meter. Then, water was
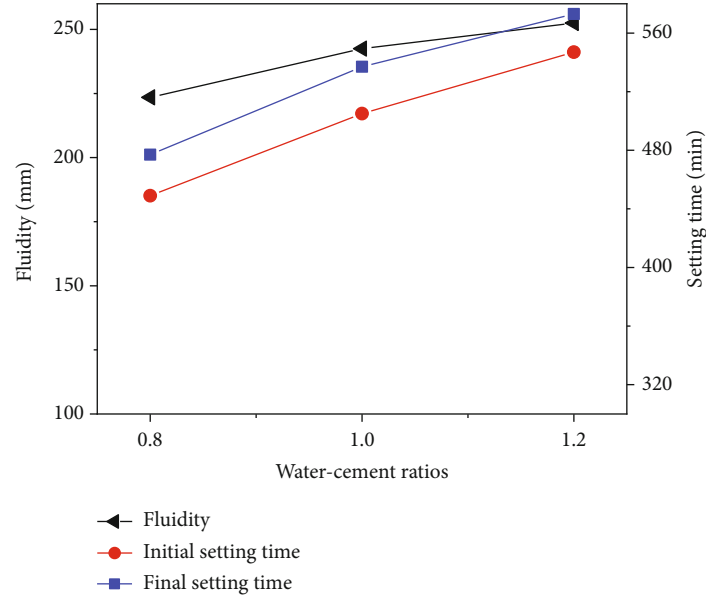
FIGURE 6: Effect of water–cement ratio on material setting time and fluidity.
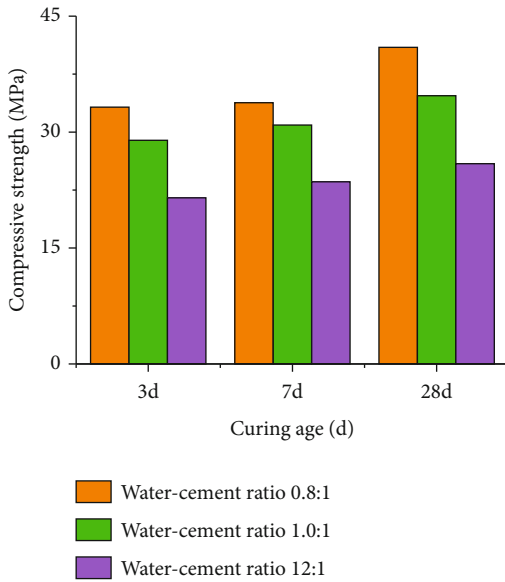

FIGURE 7: Effect of water–cement ratio on material strength.

separately added to the new borehole sealing material, which was evenly mixed poured into test molds, and placed in the curing box for curing after being leveled. Finally, the initial and final setting times of the material were measured according to the national standard (Figure 4).

Different materials were added to pure cement and mixed to form cement slurries. After molding, the initial volume was recorded as V1. The volume was read at corresponding time intervals, and the expansion rate was tested for two months. The volume was recorded as V_n, and the expansion rate of the test block was calculated with the following for-

mula. The expansion rate was calculated according to the following formula:

$$\varepsilon_t = \frac{V_n - V_1}{V_1} \times 100\%. \tag{1}$$

The sample strength test utilized the standard cement mortar strength inspection method (GB/T50080-2016), with an RMT uniaxial press used to test the compressive strength of samples with different ages (Figure 5). The specific experimental steps are as follows:

(1) Wipe clean the surface of the specimen after curing

(2) Place the test piece in the testing machine. During the compressive strength test, the pressure surface of the test piece should be perpendicular to the top surface. The center of the test piece should be aligned with the center of the lower pressure plate of the testing machine

(3) During the test, the load should be applied continuously and evenly, and the loading speed should be 0.3-0.5 MPa/s

(4) When the test piece is close to failure and begins to deform rapidly, stop adjusting the switch of the testing machine until it fails. Then, record the failure load

After obtaining the optimal ratio of admixtures through the single factor and orthogonal experiments, the ultrafine cement raw materials and admixtures were prepared according to the optimal ratio, and the results were optimized and verified.
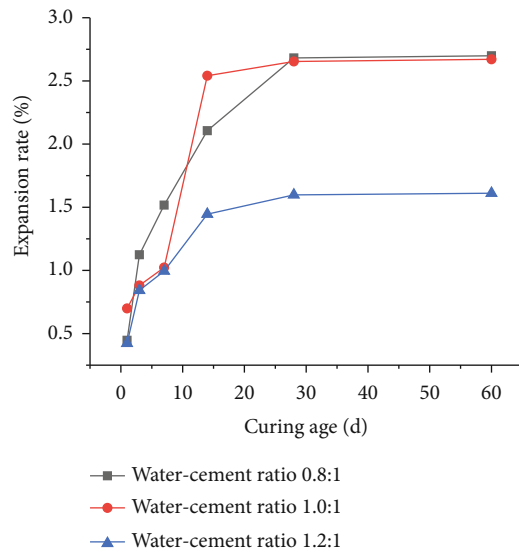
FIGURE 8: Effect of water–cement ratio on material expansion rate.

2.3. Single-Factor Experiment Method. Table 2 outlines the single-factor experimental design. While experimenting at the level of each control variable, the remaining influencing factors were controlled at fixed values. Among these, the retarder content was the ratio of the mass of the retarder to that of the ultrafine cement. The calculation method for the water-cement ratio, water-reducing agent, and expansion agent was the same as that for retarder, based on the flow of the material. The optimal value for the admixture content was determined based on the compressive strength and swelling property.

2.4. Orthogonal Experiment Method. Table 3 outlines the design of the orthogonal experiment. The water–cement ratio (A), retarder content (B), water-reducing agent content (C), and expansion agent content (D) were based on the optimal admixture content values found in the single factor experiments. In this experiment, three factors were given fixed values from the range of merit values, while the remaining factor was varied, with the resulting combinations representing a group of experiments. In order to ensure the accuracy of the results, the Box–Behnken experimental design function from the Design-Expert 8.0.5 Trial software was used. A total of 29 sets of experiments were carried out with the four factors and three levels, and the fluidity of the test block was taken as the response value.

3. Single-Factor Experiment Results and Analysis

3.1. Influence of Water–Cement Ratio on Performance of Borehole Sealing Material. The water–cement ratios selected in the experiment were 0.8, 1.0, and 1.2, and the effects of the water–cement ratio on the material properties are shown in Figures 6–8. It can be seen from Figure 6 that as the water–cement ratio increased, the fluidity and setting time of the material increased correspondingly because the consistency of the borehole sealing material decreased, and the solid

phase of cement per unit volume of material decreased. Thus, the hydration and coagulation time was relatively prolonged. From Figure 7, it can be seen that under the same curing age, the compressive strength decreases with an increase in the water–cement ratio, and under the same water–cement ratio, as the curing time increases, the compressive strength of the test block will also increase. When the water–cement ratio is 0.8, the maximum 28-day compressive strength of the material reaches 40.97 MPa. From Figure 8, it can be seen that when the water–cement ratio increases from 0.8 to 1 and the curing age increases, the expansion rate of the material first decreases, then increases, and finally remains unchanged. When the water–cement ratio continues to increase to 1.2, the expansion rate drops from the maximum of 2.699 to 1.611, which is a decrease of 40.11%. Therefore, considering the influences of the water–cement ratio on the strength, fluidity, and expansion rate of the material, a value of 0.8–1.0 is more appropriate for the water–cement ratio.

3.2. Effect of Retarder on the Properties of Sealing Material. The amounts of retarder selected in the experiment were 0.05%, 0.5%, and 1.5%. As shown in Figure 9, as the amount of retarder increases, the fluidity of the borehole sealing material continues to decrease, and the setting time increases with the retarder. This occurs because the retarder inhibits the crystallization nucleation process of the hydration product of the cement material, and it is adsorbed on the cement particles, which has a retarding effect. From Figure 10, it can be seen that at the same age, as the content of retarder increases, the strength of the material will first decrease and then increase. The compressive strength of the material was the highest when the retarder content is 0.05%, but decreased when the retarder content increased. It can be seen from Figure 11 that with an increase in retarder content, the expansion rate of the material gradually decreases. After a curing period of 30 days, the expansion rate changed more smoothly, and it expanded when the retarder content was 0.05%. The maximum rate was 2.671%. Considering on-site application and cost control, a 0.05% retarder content would be appropriate.

3.3. Influence of Water-Reducing Agent on Performance of Borehole Sealing Material. The amounts of water-reducing agent selected in the experiment were 0.2%, 0.5%, and 0.8%. As seen in Figure 12, the fluidity and setting time of the material increase with the amount of water-reducing agent. When the amount of water-reducing agent is 0.5%, this increasing trend slows down. From Figure 13, it can be seen that the contribution of the amount of water-reducing agent to the compressive strength of the test block is not always proportional. When the amount of water-reducing agent reached 0.8%, the compressive strength decreased. This occurred because the water-reducing effect reached saturation after exceeding the saturated content of PCE (0.5%), but the PCE gradually introduced a certain amount of bubbles, with more air bubbles introduced when more water-reducing agent was added. This led to more cement stone structural defects easily forming after the slurry was hydrated and hardened, resulting in small fluctuations in the mechanical properties. When
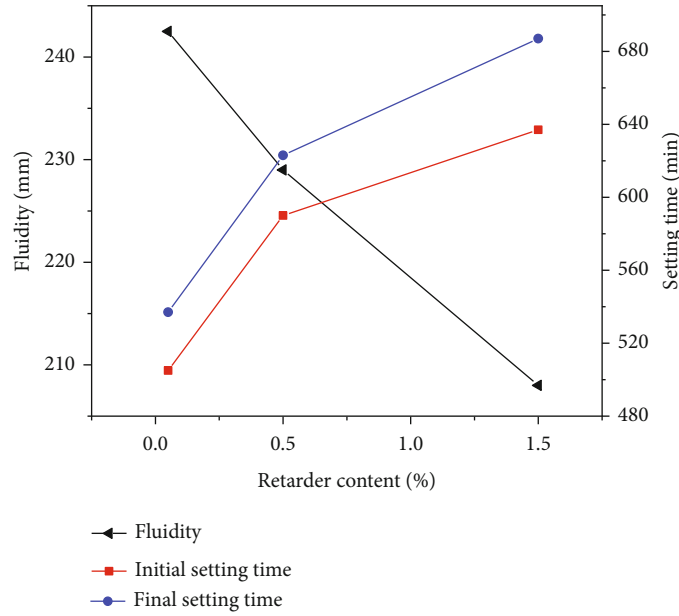
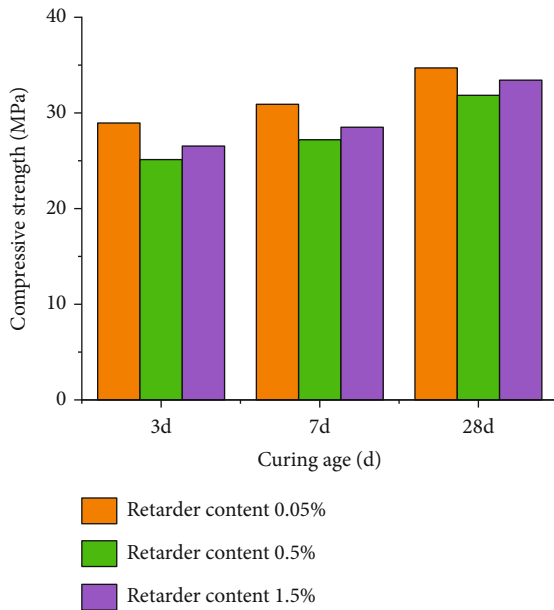FIGURE 9: Effect of amount of retarder on setting time and fluidity of material.

FIGURE 10: Effect of retarder content on material strength.

the water-reducing agent content was 0.5%, the 28-day compressive strength was 34.701 MPa. It can be seen from Figure 14 that the change law of the expansion rate is similar to that of the strength, showing a trend of increasing and decreasing. Considering the influence of the water-reducing agent on the expansion rate, strength, etc., the best dosage for the water-reducing agent was approximately 0.5%.

3.4. Influence of Expansion Agent on Performance of Borehole Sealing Material. The amounts of expansion agent selected in the experiment were 5%, 10%, and 15%. It can be seen from Figure 15 that with an increase in the amount of expansion agent, the fluidity and setting time of the test block decreased.

From Figure 16, it can be seen that with an increase in the expansion agent dosage, the compressive strength of the material first slightly increases and then decreases. This is because the expansion agent HCSA promotes the growth of needle-shaped ettringite AFt crystals in the early stage, which increases the strength. However, too much expansion agent was not conducive to the formation of strength [27]. From Figure 17, it can be seen that the expansion rate of the test block increases with the increase in the expansion agent. However, after curing for 14 days, the surface of the test block with an expansion agent content of 15% has obvious cracks (as shown in Figure 18). During the actual sealing process, new air leakage channels will be produced, which is not conducive to the sealing of the drainage borehole, resulting in a decrease in the gas concentration of the drainage borehole. Therefore, the best dosage for the expansion agent is approximately 10%.

4. Orthogonal Experiment Results and Analysis

4.1. Model Establishment. The range analysis gave the best ratio for single-objective optimization, but in the actual application process, the compressive strength, fluidity, and expansion rate need to be comprehensively considered. Thus, multiobjective nonlinear formulation optimization is required to determine the optimal matching ratio. In the orthogonal experiment results listed in Table 4, the water–cement ratio, retarder content, water-reducing agent content, and expansion agent content are independent variables A, B, C, and D, respectively. This study conducted a response surface analysis of the liquidity. First, it was necessary to select a suitable model to fit the results, and the results of the orthogonal experiment (listed in Table 5) were input into the Design-Expert 8.0.5 software to fit different models. The fitting results are listed in Table 4. The Design-Expert software recommended the use of linear equation models and
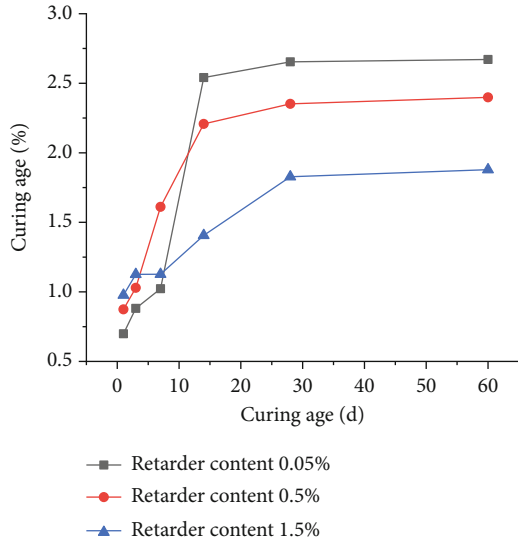
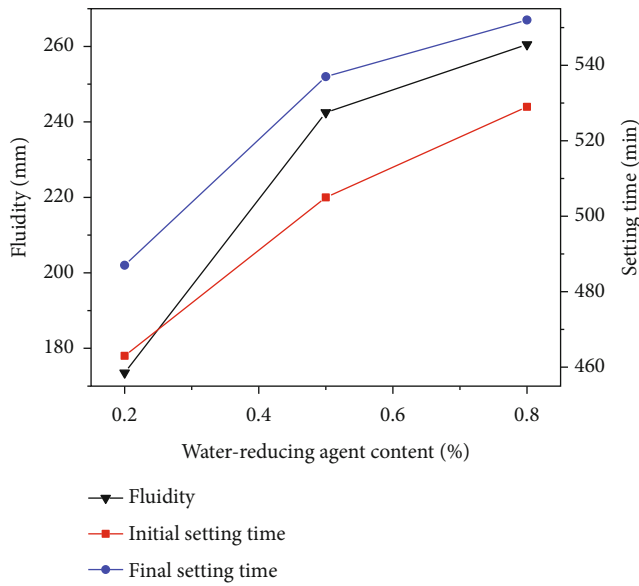Figure 11: Effect of amount of retarder on expansion rate of material.

Figure 12: Effect of water-reducing agent on material setting time and fluidity.

Figure 13: Effect of water-reducing agent on material strength.
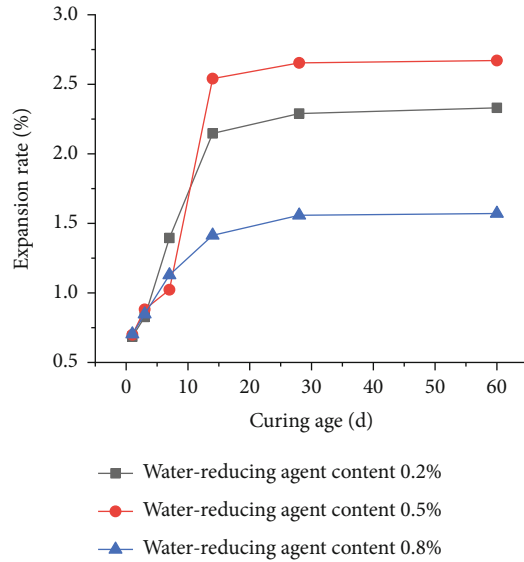
Figure 14: Effect of water-reducing agent on material expansion rate.

quadratic equation models, which had better fits than other models. It can be seen from Table 4 that the sum of the squared prediction residuals is low in several models; however, the R^2 value of the linear model is 0.685, which is smaller than the R^2 value of the quadratic equation model (0.9144), indicating that the model's correlation with the experimental results is low. Thus, the model is inaccurate. The Adj R^2 value of the linear model is small compared with that of the quadratic equation model, indicating that the model still needs further development. Based on these results, the experiment initially selected the quadratic equation model for fitting.
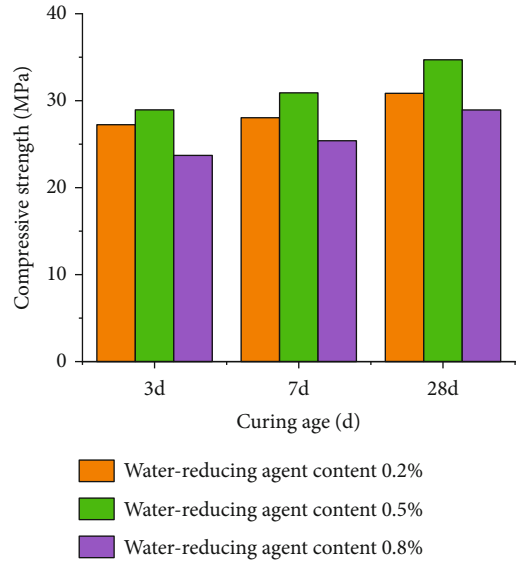
4.2. Variance Results and Significance Tests.

From Table 6, it can be seen that the F value of the model is 10.69, the Prob $> F$ value is less than 0.0001, and the correction coefficient of determination (Adj R^2) is 0.8289, which shows that the model fits the data well and the experimental error is small. From the significance test, it can be seen that the factors had the following order of significance: C (water − reducing agent) > A (water − cement ratio) > B (retarder) > D (expansion agent). The factor combinations had the following order: AC (water − cement ratio, water − reducing agent) > CD (water − reducing agent, expansion agent) > BC (retarder, water − reducing agent) > AD (water − cement ratio , expansion agent) > AB (water − cement ratio, expansion agent) > BD (retarder, expansion agent). Among these, the
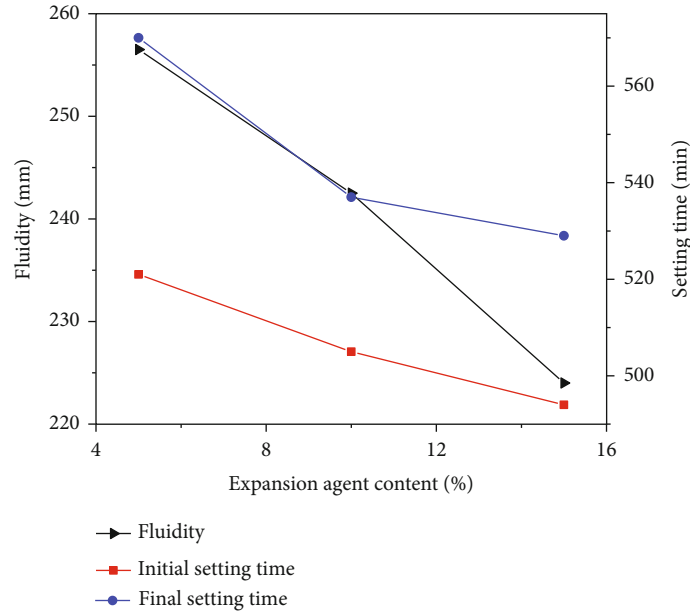
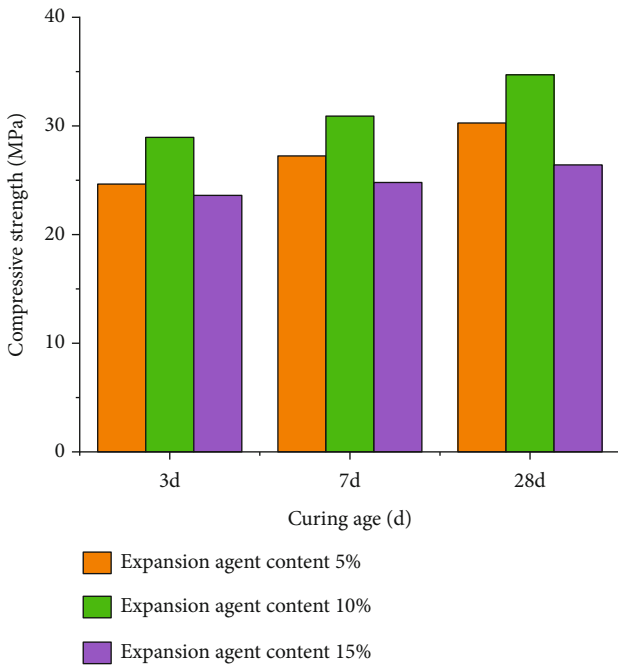FIGURE 15: Effect of expansion agent on material setting time and fluidity.

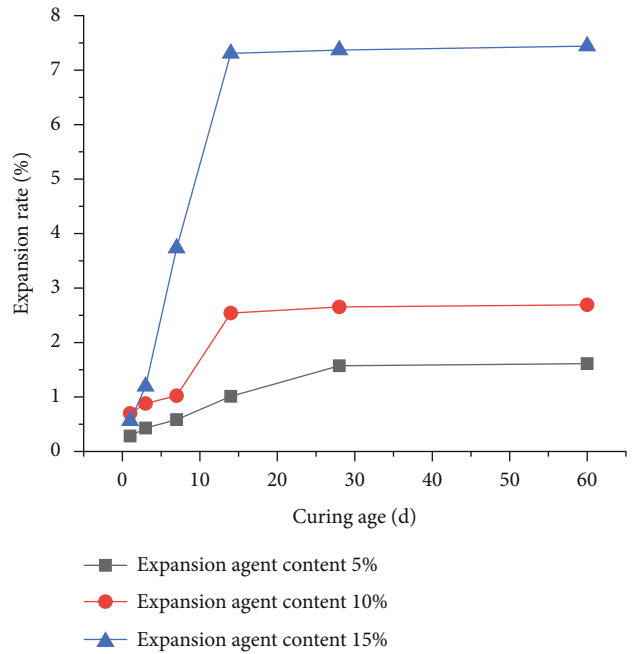FIGURE 16: Effect of expansion agent on material strength.

FIGURE 17: Effect of expansion agent on material expansion rate.

Prob > F value of the C factor was less than 0.0001, which indicated that the index was extremely significant, and the Prob > F values of factors A and B were less than 0.005, which indicated that these two indicators were significant; the interaction of AC was the most significant, and the interaction of BD was the least significant.

4.3. Response Surface Analysis. The response surface drawn according to the binomial polynomial regression equation was a three-dimensional surface obtained by the interaction of the response values of the independent variables. The

response value (liquidity) could be predicted and optimized, and any two factors could also be adjusted to analyze their interaction and obtain the interaction rules. It was possible to determine when any two of the four factors (A (water–cement ratio), B (retarder content), C (water-reducing agent content), and D (expansion agent content)) remained unchanged by the interaction and laws of the other two factors.

Figure 19 shows the effect of the water–cement ratio and water-reducing agent on the fluidity results. It can be seen from Figure 19 that the fluidity varies greatly with the

FIGURE 18: Effect of different dilatant dosages on test block.

TABLE 4: Comprehensive statistical analysis of multiple models.

Source	Std. dev.	R-squared	Adjusted R-squared	Predicted R-squared	PRESS	
Linear	17.95	0.6850	0.6324	0.5231	11701.95	Suggested
2FI	16.86	0.7915	0.6757	0.3841	15111.63	
Quadratic	12.25	0.9144	0.8289	0.5072	12092.52	Suggested
Cubic	5.98	0.9912	0.9592	-0.2605	30927.00	

TABLE 5: Orthogonal test results.

No	A	B/%	C/%	D/%	R3d/MPa	R7d/MPa	R28d/MPa	Fluidity/mm	Initial setting time/min	Final setting time/min	Expansion rate/%
1	0.8	0.03	0.4	9	29.899	32.069	41.597	213.5	440	469	1.897
2	0.8	0.04	0.5	9	37.697	38.477	42.833	226	419	437	2.032
3	0.8	0.04	0.4	10	30.986	32.991	38.969	190.5	410	430	3.281
4	0.8	0.04	0.3	9	33.997	35.01	39.021	199	406	443	1.931
5	0.8	0.04	0.4	8	39.918	42.197	41.398	185.5	431	458	1.593
6	0.8	0.05	0.4	9	31.652	34.133	37.256	207.5	461	490	1.821
7	0.9	0.03	0.5	9	28.479	32.141	36.966	242	343	376	1.898
8	0.9	0.03	0.4	10	26.943	28.511	34.981	218.5	344	368	2.471
9	0.9	0.03	0.4	8	30.931	32.871	38.996	234	416	438	1.614
10	0.9	0.03	0.3	9	27.696	31.233	37.061	179	337	370	1.521
11	0.9	0.04	0.4	9	28.601	30.381	36.983	193	430	456	2.053
12	0.9	0.04	0.4	9	28.601	30.381	36.983	193	430	456	2.053
13	0.9	0.04	0.3	10	31.239	32.011	34.882	153.5	424	449	2.329
14	0.9	0.04	0.4	9	28.601	30.381	36.983	193	430	456	2.053
15	0.9	0.04	0.5	8	34.312	38.021	37.409	212	437	463	1.589
16	0.9	0.04	0.5	10	31.213	32.997	34.411	243	422	444	2.809
17	0.9	0.04	0.3	8	32.986	36.021	37.311	183.5	431	457	1.621
18	0.9	0.04	0.4	9	28.601	30.381	36.983	193	430	456	2.053
19	0.9	0.04	0.4	9	28.601	30.381	36.983	193	430	456	2.053
20	0.9	0.05	0.3	9	25.896	28.033	33.767	153.5	482	518	1.621
21	0.9	0.05	0.5	9	26.062	29.133	36.761	247	360	395	1.812
22	0.9	0.05	0.4	10	26.993	27.012	33.761	167	365	393	2.597
23	0.9	0.05	0.4	8	28.922	30.41	34.562	185	490	525	1.531
24	1	0.04	0.3	9	27.664	29.008	33.678	179	420	454	1.986
25	1	0.03	0.4	9	26.295	28.091	32.019	240	349	376	1.778
26	1	0.04	0.4	10	26.513	27.978	28.072	230	359	386	2.093
27	1	0.05	0.4	9	23.997	27.843	31.907	229.5	475	503	1.803
28	1	0.04	0.4	8	28.911	31.036	38.213	207.5	439	463	1.302
29	1	0.04	0.5	9	27.476	29.989	33.778	280	422	457	1.889

Table 6: Response surface quadratic model and analysis of variance results.

Source	Sum of squares	df	Mean square	F	Prob > F
Model	22436.79	14	1602.63	10.69	<0.0001
A	1728.00	1	1728.00	11.52	0.0044
B	1575.52	1	1575.52	10.51	0.0059
C	13500.52	1	12838.02	90.03	<0.0001
D	2.08	1	2.08	0.014	0.9078
AB	5.06	1	5.06	0.034	0.8569
AC	1369.00	1	1369.00	9.13	0.0092
AD	76.56	1	76.56	0.51	0.4866
BC	232.56	1	232.56	1.55	0.2334
BD	1.56	1	1.56	0.010	0.9201
CD	930.25	1	930.25	6.20	0.0259
A2	2200.05	1	2200.05	14.67	0.0018
B2	582.84	1	582.84	3.89	0.0688
C2	327.37	1	327.37	2.18	0.1617
D2	95.32	1	95.32	0.64	0.4386
Residual	2099.40	14	149.96		
Lack of fit	2099.40	10	209.94		
Pure error	0.000	4	0.000		
Cor total	24536.19	28			

water–cement ratio or water-reducing agent, and the response surface is steep at this time. As reflected in the contour map, the contour lines are dense. The rapid color change in the contour map also proves that the slope of the response surface is large. This indicates that the water–cement ratio and interaction of the water-reducing agent have a significant impact on the response value, which is consistent with the previous variance analysis results for each item. The two factors of the ash ratio and water-reducing agent have a more significant influence on the test results. Because with the gradual increase of the water-cement ratio, the free water content in the cement slurry gradually increases, the free water has a diluting and dispersing effect on the flocculent structure, the large-volume floccules gradually separate and become smaller, and the small-volume floccules are gradually separated disassembly and separation, so when the water-cement ratio is small, the initial apparent viscosity of the cement slurry is greater. When the water-cement ratio is 0.5 to 0.8, with the gradual increase of the water-cement ratio, on the one hand, more sufficient water molecules are provided for the physical and chemical reactions of the cement slurry, and the floc structure is produced. More effective reaction conditions, on the other hand, the increase of free water molecules causes the flocs to decompose into smaller-structured flocs, which reduces the dispersion resistance. At the same time, the free water molecules also play a better lubricating effect between the flocs. When the water-cement ratio is greater than 1.0 (the water-cement ratio is 1.0 and 2.0), because the free water content reaches a saturated state, the free water has little effect on the physical and chemical reactions of the slurry, and the free water has

small. The decomposition of substances and the lubrication of flocs are the main influencing factors.

Figure 20 shows the effect of the water-reducing agent and expansion agent on the fluidity results. It can be seen from Figure 20 that when the water-reducing agent and expansion agent are taken at the upper limits of their selected level ranges, the fluidity change trend is relatively steep, indicating that the interaction between the time-reducing agent and expansion agent has a significant impact on the response value. The contour distribution trend is related to the factor level, and there is a certain distortion in the three-dimensional surface graph. The interaction of these two factors affects the particle flow, and the dense contour lines on the abscissa also indicate that the water-reducing agent has a greater impact on fluidity. Because the polycarboxylic acid water reducer can promote the hydration process of cement, the total amount of CSH gel and Ca(OH) 2 in the cement stone can be increased, and the polycarboxylic acid water reducer can greatly reduce the particles of CSH. It can increase the degree of polymerization of the gel, and the polycarboxylic acid-based water reducing agent can increase the degree of polymerization of silicon-oxygen tetrahedron in the CSH of the hydration product.

Figure 21 shows the effect of the retarder and water-reducing agent on the fluidity results. It can be seen from Figure 21 that the contour lines on the ordinate are denser, while the contour lines on the abscissa are sparse, indicating that the retarder has a greater impact on fluidity. When the upper limit of the content of the retarder is used, the response surface is relatively smooth, indicating that the retarder has a certain influence on the fluidity, but the range of this influence is small.

Figure 22 shows the effect of the water–cement ratio and expansion agent on the fluidity results. It can be seen from Figure 22 that the contour lines of the ordinate are sparse, and the contour lines of the abscissa are dense, indicating that the water–cement ratio has a greater impact on the fluidity. The expansion agent has little effect on the fluidity; the response surface is relatively smoother, indicating that the interaction of the two factors has a certain impact on the fluidity, but the range of this influence is small. When using the upper limits of the two factors, the response surface is steep, indicating that the interaction of the two factors has the greatest impact on the liquidity at this time.

Figure 23 shows the effect of the water–cement ratio and retarder on the fluidity results. The shape of the contour reflects the strength of the interaction effect. A circle indicates that the interaction of the two factors is not significant, while an ellipse shows the opposite. It can be seen from Figure 23 that the distribution of the abscissa contour lines is denser than that on the ordinate, indicating that the influence of the water–cement ratio on the response value is more significant than that of the retarder. The pattern change law is similar to the response obtained by the two-factor analysis of variance in the figure. The influence law of the value is the same, and the graph has a certain distortion. When the water–cement ratio is at the upper limit and the retarder is at
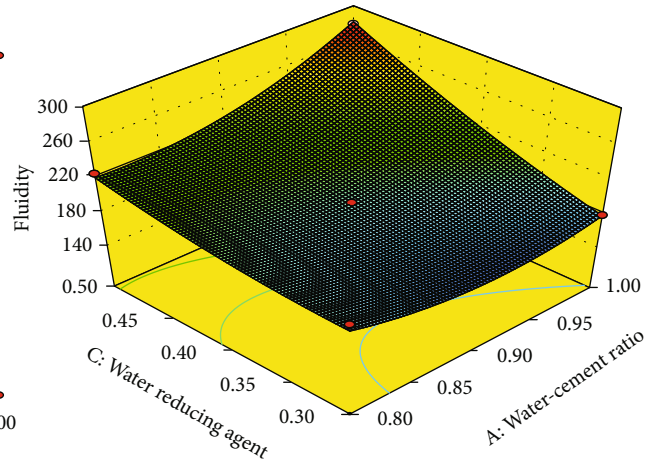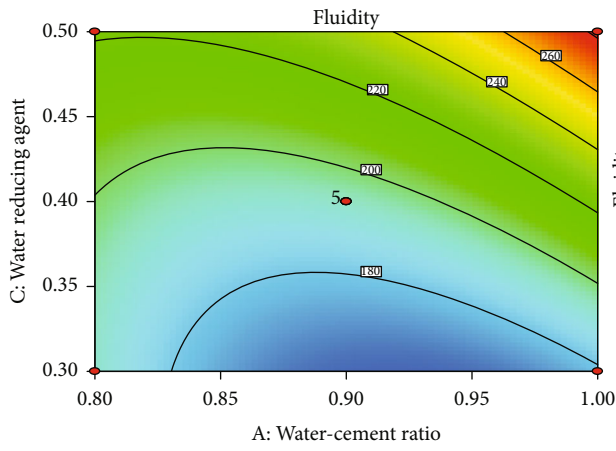
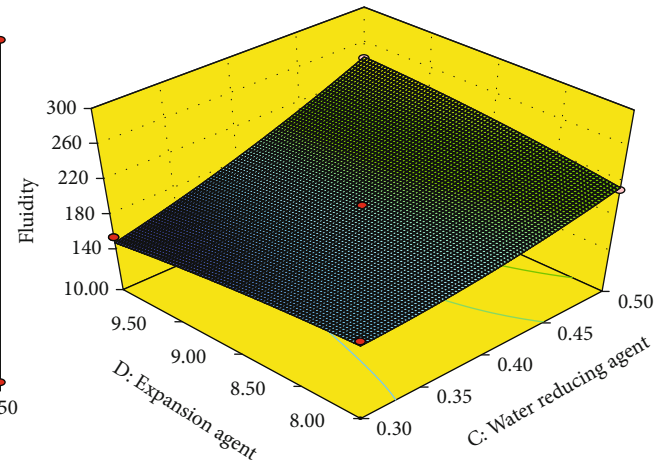FIGURE 19: Effect of water–cement ratio and water reducer on fluidity.
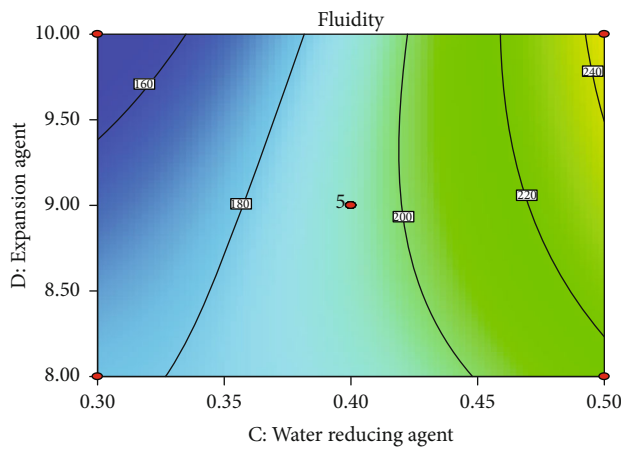

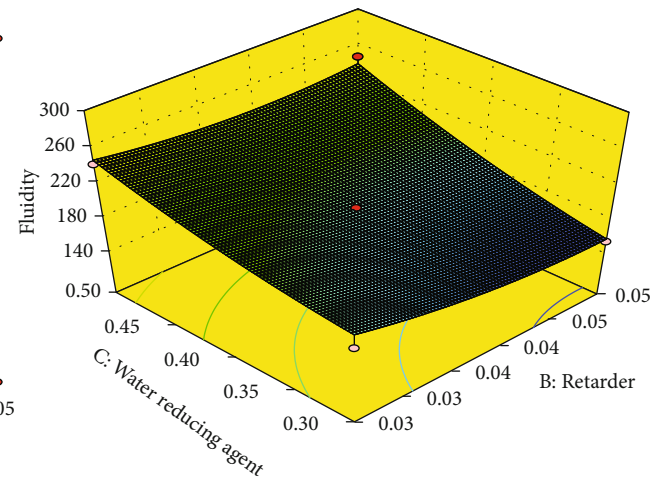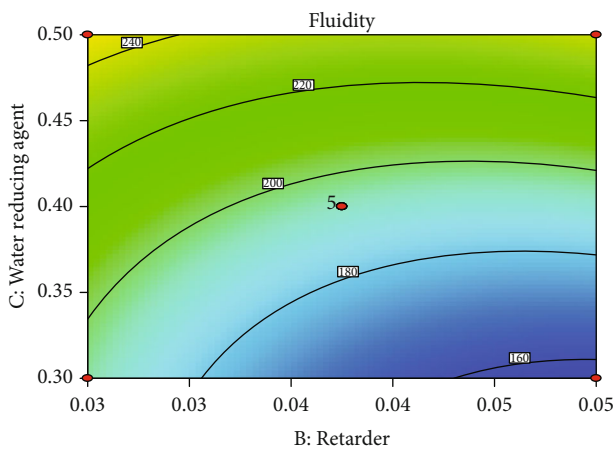FIGURE 20: Effect of water-reducing agent and expansion agent on fluidity.

FIGURE 21: Effect of retarder and water-reducing agent on fluidity.
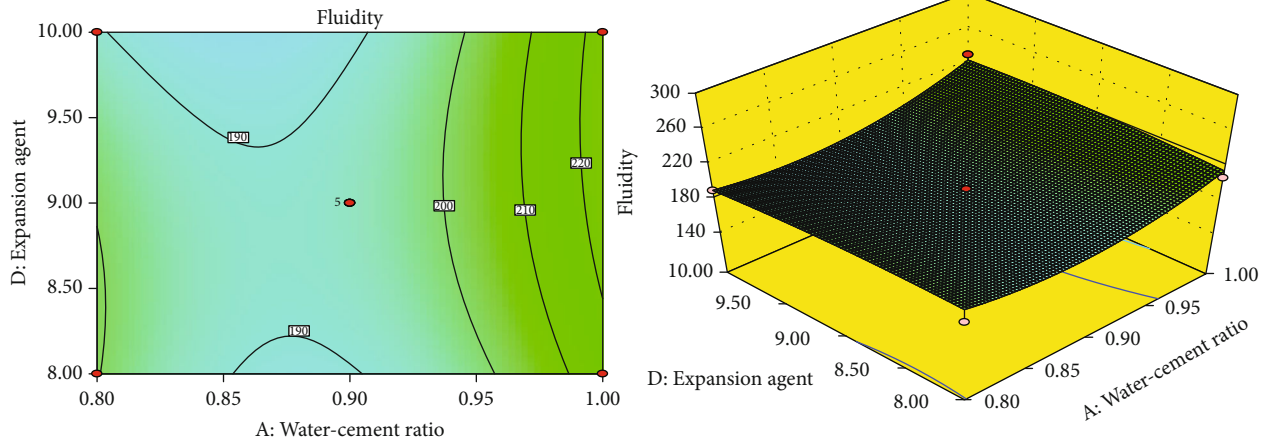
FIGURE 22: Effect of water–cement ratio and expansion agent on fluidity.
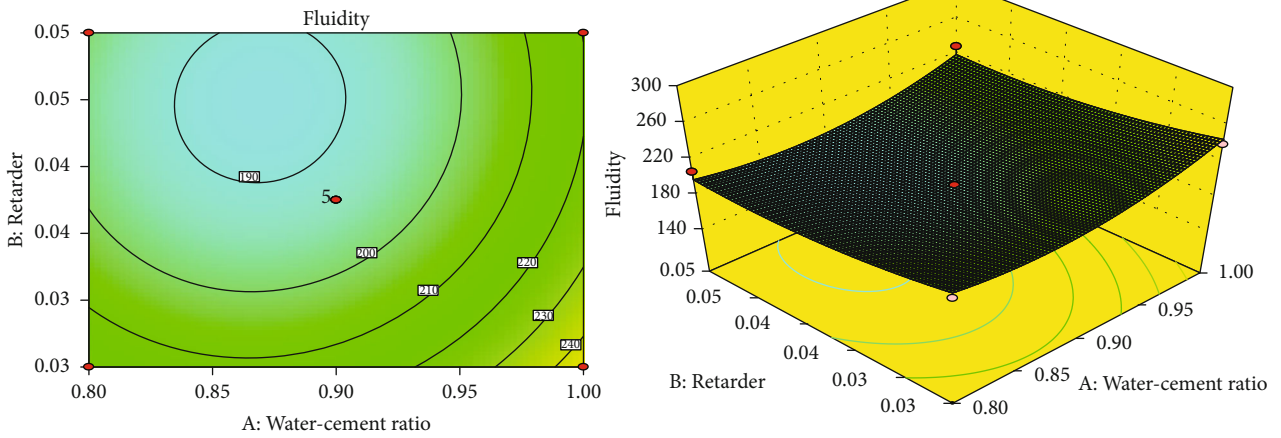

FIGURE 23: Effect of water–cement ratio and retarder on fluidity.
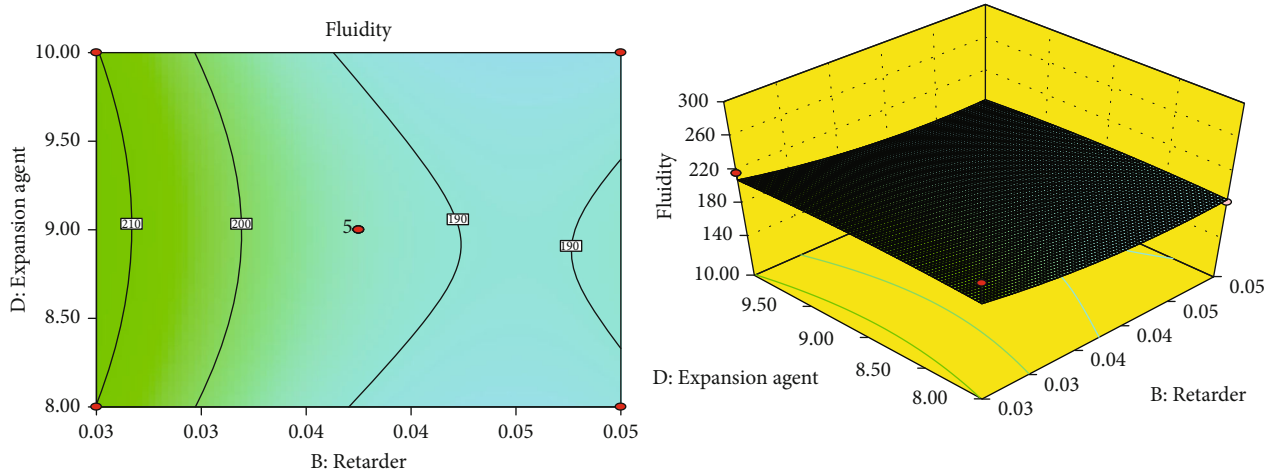

FIGURE 24: Effect of retarder and expansion agent on fluidity.

the lower limit, the response surface is steep, but the overall response surface is relatively flat, indicating a certain interaction between the two factors, but the effect is small.

Figure 24 shows the effect of the retarder and expansion agent on the fluidity results. As shown in Figure 24, the contour lines on the abscissa are dense, while the contour lines on the ordinate are sparse, indicating that the influence of

Table 7: Optimization scheme and results.

No	Water-cement ratio	Experimental optimization ratio			Forecast liquidity/mm	Measured liquidity/mm	Error/%
		Retarder/%	Water reducing agent/%	Expansion agent/%			
1	1	0.03	0.5	8.81	288.494	288	-0.518
2	0.99	0.03	0.49	9.11	287.832	287	-0.289
3	0.98	0.04	0.5	9.98	287.561	287.5	-0.021
4	1	0.03	0.49	9.06	288.624	286.5	-0.736
5	0.97	0.03	0.49	9.98	283.282	283.5	0.077
6	0.98	0.03	0.49	9.82	287.186	287	-0.065

the coagulant on the fluidity is greater than that of the expansion agent. This is consistent with the results of the analysis of variance, and the response surface is the smoothest when the retarder interacts with the expansion agent, indicating that the interaction between the retarder and expansion agent has the least significant effect on the fluidity. This is due to the hydration reaction of the mineral components in the expansion agent to produce more AFT, which leads to the increase of hydration products in the cement hydration system, the increase of system consistency, and the decrease of fluidity. This is due to the hydration reaction of the mineral components in the expansion agent to produce more AFT, which leads to the increase of hydration products in the cement hydration system, the increase of system consistency, and the decrease of fluidity.

4.4. Parameter Optimization and Verification. The Design-Expert software was used for a further analysis of the experimental results, using the fluidity as the optimization index to obtain the optimized experimental program by selecting the first six groups of optimized experimental programs and verifying them, as shown in Table 7.

It can be seen from Table 7 that when using the optimized ratio recommended by the Design-Expert 8.0.5 software, the maximum absolute error between the predicted value of liquidity and the actual value obtained by an actual measurement in the laboratory was only 0.736%, indicating that the model was relatively reliable. Taking into account the operability and simplicity of on-site grouting, when the water–cement ratio is relatively small, the thickness of the borehole sealing material is too large. This makes grouting more difficult, and it is prone to blockage. The retarder has a certain viscosity to increase the consistency of the material. Thus, it is appropriate to reduce the amount of retarder to increase the fluidity. The comprehensive expansion rate, fluidity, and strength were considered to select and optimize the experimental conditions as follows: water-reducing agent of 0.5%, retarder of 0.03%, water–cement ratio of 1, and expansion agent of 8%.

5. Conclusions

The results obtained in this study made it possible to draw the following conclusions.

(1) It can be seen from the experimental results that as the water-cement ratio increases, the fluidity and setting time of the material increase correspondingly. Under the same curing age, the compressive strength decreased with the water-cement ratio increased; with an increase in the retarder content, the fluidity of the borehole sealing material continued to decrease, and the setting time increased with an increase in the retarder content. At the same age, with an increase in the retarder content, the strength of the material first decreased and then increased. As the amount of water-reducing agent increased, the fluidity and setting time of the material increased. When the amount of water-reducing agent was 0.5%, this increasing trend slowed down and the contribution of the amount of water-reducing agent to the compressive strength of the test block was not always proportional. When the amount of water-reducing agent reached 0.8%, the compressive strength of the test block decreased. With the amount of expansion agent increased, the fluidity and setting time of the test block decreased. With the amount of expansion agent increased, the compressive strength of the material first increased slightly and then decreased

(2) With ultrafine cement as the base material, an expansion agent, polycarboxylic acid water-reducing agent, and retarder were added to develop a sealing material to meet the performance requirements of fluidity and expansion

(3) Orthogonal experiments were designed using the Box–Behnken module in the Design-Expert software. Fluidity was the response value, and various test factors (water–cement ratio, water-reducing agent, retarder, and expansion agent) were established and optimized. The quadratic model of time showed a high prediction accuracy

(4) The influence of each component on the fluidity of the material was obtained using a range and variance analysis and a significance test. These had the following order: C (water – reducing agent) > A (water cement ratio) > B (retarder) > D (expansion agent)

(5) According to the response surface drawn by the binomial polynomial regression equation, the interaction

of any two factors was analyzed, and the interaction laws were obtained. These effects had the following order: AC (water – cement ratio, water – reducing agent) > CD (water – reducing agent, expansion agent) > BC (retarder, water – reducing agent) > AD (water – cement ratio, expansion agent) > AB (water – cement ratio, retarder) > BD (retarder, expansion agent)

(6) The response surface analysis method combined the single factor experiment results and the actual sealing grouting situation to obtain the best experimental conditions in this experiment: a water-reducing agent content of 0.5%, a retarder content of 0.03%, a water-cement ratio of 1, and an expansion agent content of 8%

Data Availability

The data used for conducting classifications are available from the corresponding author authors upon request.

Conflicts of Interest

The authors declared no potential conflicts of interest with respect to the research, authorship, and/or publication of this article.

Acknowledgments

References

[1] L. Yuan, "Strategic thinking of simultaneous exploitation of coal and gas in deep mining," *Journal of China Coal Society*, vol. 41, no. 1, pp. 1–6, 2016.

[2] L. Yuan and P. S. Zhang, "Development status and prospect of geological guarantee technology for precise coal mining," *Journal of China Coal Society*, vol. 44, no. 8, pp. 2277–2284, 2019.

[3] L. Fan, H. M. Zhou, and Y. H. Zhang, "Influence of microfractures on strength parameters of engineering rock mass," *Chinese Journal of Rock Mechanics and Engineering*, vol. 30, no. 1, pp. 2703–2709, 2011.

[4] M. Wtrzykowshi, P. Trtik, and B. Munch, "Plastic shrink age of mortars with shrink age reducing admixture and lightweight aggregates studied by neutron tomography," *Cement and Concrete Research*, vol. 73, pp. 238–245, 2015.

[5] F. Pelisser, B. Aimir, and L. Henriette, "Effect of the addition of synthetic fibers to concrete thin slabs on plastic shrinkage cracking," *Construction and Building Materials*, vol. 24, no. 11, pp. 2171–2176, 2010.

[6] M. Wasil, "Effect of bentonite addition on the properties of fly ash as a material for landfill sealing layers," *Applied Sciences*, vol. 10, no. 4, article 1488, 2020.

[7] P. K. De Maeijer, B. Craeye, R. Snellings et al., "Effect of ultrafine fly ash on concrete performance and durability," *Construction and Building Materials*, vol. 263, article 120493, 2020.

[8] H. M. Sujay, N. A. Nair, H. S. Rao, and V. Sairam, "Experimental study on durability characteristics of composite fiber reinforced high-performance concrete incorporating nanosilica and ultra fine fly ash," *Construction and Building Materials*, vol. 262, article 120738, 2020.

[9] E. Boghssian and L. D. Wegne, "Use of flax fibres to reduce plastic shrinkage cracking in concrete," *Cement and Concrete Research*, vol. 30, no. 10, pp. 929–937, 2008.

[10] J. Hogancamp and Z. Grasley, "The use of microfine cement to enhance the efficacy of carbon nanofibers with respect to drying shrinkage crack resistance of Portland cement mortars," *Cement and Concrete Composites*, vol. 83, pp. 269–272, 2017.

[11] H. Y. Li, Y. C. Zhang, J. Wu, X. Y. Zhang, L. W. Zhang, and Z. F. Li, "Grouting sealing mechanism of water gushing in karst pipelines and engineering application," *Construction and Building Materials*, vol. 254, article 119250, 2020.

[12] D. P. Zheng, D. M. Wang, D. L. Li, C. F. Ren, and W. C. Tang, "Study of high volume circulating fluidized bed fly ash on rheological properties of the resulting cement paste," *Construction & Building Materials*, vol. 135, pp. 86–93, 2017.

[13] Y. Liu, J. G. Han, M. Y. Li, and P. Y. Yan, "Effect of a nanoscale viscosity modifier on rheological properties of cement pastes and mechanical properties of mortars," *Construction and Building Materials*, vol. 190, pp. 255–264, 2018.

[14] C. Chen, L. Y. Peng, and Z. H. Zhang, "Performance of superfine cement-water glass double slurry and effect analysis on sand grouting," *Bulletin of the Chinese Ceramic Society*, vol. 37, no. 12, pp. 3883–3887, 2018.

[15] N. Wongkornchaowalit and V. Lertchirakarn, "Setting time and flowability of accelerated Portland cement mixed with polycarboxylate superplasticizer," *Journal of Endodontics*, vol. 37, no. 3, pp. 387–389, 2011.

[16] M. Kazuki, S. Daiki, K. Hirokatsu, and S. Etsuo, "Effect of non-adsorbed superplasticizer molecules on fluidity of cement paste at low water-powder ratio," *Cement and Concrete Composites*, vol. 97, pp. 218–225, 2019.

[17] H. Güllü, A. Cevik, K. Al-Ezzi, and M. E. Gülsan, "On the rheology of using geopolymer for grouting: a comparative study with cement-based grout included fly ash and cold bonded fly ash," *Construction and Building Materials*, vol. 196, pp. 594–610, 2019.

[18] W. Kubissa, R. Jaskulski, and M. Grzelak, "Torrent air permeability and sorptivity of concrete made with the use of air entraining agent and citric acid as setting retardant," *Construction and Building Materials*, vol. 268, article 121703, 2021.

[19] T. Kim, K. Y. Seo, C. Kang, and T. K. Lee, "Development of eco-friendly cement using a calcium sulfoaluminate expansive agent blended with slag and silica fume," *Applied Sciences*, vol. 11, no. 1, p. 394, 2021.

[20] D. S. Vijayan and D. Parthiban, "Effect of solid waste based sta-bilizing material for strengthening of expansive soil- a review," *Environmental Technology & Innovation*, vol. 20, article 101108, 2020.

[21] H. Kabir and R. D. Hooton, "Evaluating soundness of concrete containing shrinkage-compensating MgO admixtures," *Construction and Building Materials*, vol. 253, article 119141, 2020.

[22] I. Cavusoglu, E. Yilmaz, and A. O. Yilmaz, "Additivity effect on properties of cemented coal fly ash backfill containing water-reducing admixtures," *Construction and Building Materials*, vol. 267, article 121021, 2021.

[23] M. Kioumarsi, F. Azarhomayun, M. Haji, and M. Shekarchi, "Effect of shrinkage reducing admixture on drying shrinkage of concrete with different w/c ratios," *Materials*, vol. 13, no. 24, article 5721, 2020.

[24] O. U. Izevbekhai, W. M. Gitari, N. T. Tavengwa, W. B. Ayinde, and R. Mudzielwana, "Response surface optimization of oil removal using synthesized polypyrrole-silica polymer com-posite," *Molecules*, vol. 25, no. 20, article 4628, 2020.

[25] B. S. Mohammed, V. C. Khed, and M. S. Liew, "Optimization of hybrid fibres in engineered cementitious composites," *Construction and Building Materials*, vol. 190, pp. 24–37, 2018.

[26] N. U. Kockal and T. Ozturan, "Optimization of properties of fly ash aggregates for high-strength lightweight concrete pro-duction," *Materials & Design*, vol. 32, no. 6, pp. 3586–3593, 2011.

[27] J. Carette, B. Delsaute, N. Milenkovic, J. P. Lecomte, M. P. Del-plancke, and S. Staquet, "Advanced characterisation of the early age behaviour of bulk hydrophobic mortars," *Construction and Building Materials*, vol. 267, article 120904, 2021.